HHS Public Access

Author manuscript

Eur Radiol. Author manuscript; available in PMC 2020 October 01.

Published in final edited form as:

Eur Radiol. 2019 October ; 29(10): 5298–5306. doi:10.1007/s00330-019-06115-w.

Can amide proton transfer-weighted imaging differentiate tumor grade and predict Ki-67 proliferation status of meningioma?

Hao Yu[1,2,#], **Xinrui Wen**[3,#], **Pingping Wu**[4], **Yueqin Chen**[1], **Tianyu Zou**[5], **Xianlong Wang**[2], **Shanshan Jiang**[2,6], **Jinyuan Zhou**[6], **Zhibo Wen**[2]

[1]Department of Radiology, Affiliated Hospital of Jining Medical University, Jining Medical University, Guhuai Road No.89, Rencheng District, Jining, Shandong, 272029

[2]Department of Radiology, Zhujiang Hospital, Southern Medical University, Gongye Road M No. 253, Haizhu District, Guangzhou, Guangdong, 510282

[3]Department of Neurology, Zhujiang Hospital, Southern Medical University, Gongye Road M No. 253, Haizhu District, Guangzhou, Guangdong, 510282, China.

[4]Department of Clinical Laboratory, Jining NO. 1 People's Hospital, 6 Jiankang Road, Jining, 272011, China.

[5]Department of Radiology, Weihai Municipal Hospital, Heping Road M No.70, Weihai, Shandong, 264200, China.

[6]Division of MR Research, Department of Radiology, Johns Hopkins University School of Medicine, 600N. Wolfe Street, Park 336, Baltimore, Maryland 21287, USA

Abstract

Objectives: To determine the utility of the amide proton transfer-weighted MR imaging in differentiating the WHO grade and predict proliferative activity of meningioma.

Methods: Fifty-three patients with WHO grade I meningiomas and twenty-six patients with WHO grade II meningiomas underwent conventional and APT-weighted sequences on a 3.0 Tesla MR before clinical intervention. The APT-weighted (APTw) parameters in the solid tumor region were obtained and compared between two grades using the t-test, the receiver operating characteristic (ROC) curve was used to assess the best parameter for predicting the grade of

*Corresponding author: Please address correspondence to Zhibo Wen, MD. Professor Department of Radiology, Zhujiang Hospital, Southern Medical University, Gongye Road M No.253, Haizhu District, Guangzhou, Guangdong, 510282, China. Phone: +86-13802914951; 86-20-61643461., zhibowen@163.com.

#These authors have contributed equally to this work.

Conflict of interest:
The authors of this manuscript declare no relationships with any companies, whose products or services may be related to the subject matter of the article.

Statistics and Biometry:
No complex statistical methods were necessary for this paper.

Informed Consent:
Written informed consent was obtained from all subjects (patients) in this study.

Ethical Approval:
Institutional Review Board approval was obtained.

meningiomas. Pearson's correlation coefficient was calculated between the $APTw_{max}$ and Ki-67 labeling index in meningiomas.

Results: The $APTw_{max}$ and $APTw_{mean}$ values were not significantly different between WHO grade I and grade II meningiomas (*P=0.103* and *P=0.318*). The $APTw_{min}$ value was higher and the $APTw_{max-mim}$ value was lower in WHO grade II meningiomas than in WHO grade I tumors. (*P=0.027* and *P=0.019*). But the $APTw_{min}$ was higher and the $APTw_{max-min}$ was lower in microcystic meningiomas than in WHO grade II meningiomas(*P= 0.001* and *P=0.006*). The $APTw_{min}$ combined with $APTw_{max-min}$ showed the best diagnostic performance in predicting the grade of meningiomas with an AUC of 0.772. The $APTw_{max}$ value was positively correlated with Ki-67 labeling index (r=0.817, *P*<0.00l) in meningiomas, the regression equation for the Ki-67 labeling index (%) (Y) and $APTw_{max}$ (%)(X) was Y=4.9×X-12.4 (R^2 =0.667, *P<0.001*).

Conclusion: As a noninvasive imaging method, the ability of APTw-MR imaging in differentiating the grade of meningiomas is limited, but the technology can be used to predict the proliferative activity of meningioma.

Keywords

Magnetic resonance imaging; Amide proton transfer; Meningioma; Tumor grading; Cell proliferation

---

According to CBTRUS, there are 15 subtypes of meningiomas, constitute approximately 36.7% of all primary central nervous system neoplasms [1]. Most meningiomas are benign tumor classified as WHO grade I and the recurrence are infrequent, nearly 5% are WHO grade II/III tumors which behave more aggressively[2]. Surgical resection is the first choice for the treat of meningioma, but surgery is invasive treatment, for most of benign meningiomas with diameter <3cm, close follow-up is a better management [3]. Ki-67 is a proliferation-related nuclear antigen that indicates the speed of tumor growth[4]. Previous studies have suggested that meningiomas with Ki-67 labeling index ≥ 3% are prognostic for an increased risk of progression and recurrence[5]; Therefore, differentiate meningioma grade and predict Ki-67 proliferation status preoperatively would be helpful for therapeutic planning.

Conventional and advanced MRI techniques can provide sufficient information to diagnose a meningioma. However, it has a limited diagnostic specificity in differentiating meningioma grade and predicting proliferation potential[6–11]. Amide proton transfer-weighted (APTw) MRI is a novel molecular MRI technique based on chemical exchange-based saturation transfer (CEST) and applied to imaging through the exchange between amide protons of mobile proteins and protons of bulk water [12]. The APTw signal is mainly related to cell density and endogenous mobile proteins [13; 14]. As an imaging biomarker, worthwhile results have been reported across various research, in grading glioma [15; 16]; distinguishing treatment effects from tumor recurrence[17; 18]; differentiating glial neoplasms from other intracranial tumor[13; 19]; distinguishing cancerous tissues in the prostate and breast[20; 21] and in other non-oncological diseases [22–24]. However, this technique is rarely used in meningioma, and only one investigator has reported using APTw MR imaging to assess

meningioma[25]. Therefore, the purpose of this study was to determine the utility of APT-weighted MRI in differentiating the tumor grade and proliferative activity of meningioma

Materials and Methods

Study population

The institutional review board of our hospital approved this retrospective study, and each patient signed the informed consent. 93 patients suspected meningiomas were recruited and underwent conventional and APT-weighted MRI from May 2014 to June 2018. 86 patients were pathologically diagnosed as meningiomas. 7 patients were excluded for whom poor quality APTw images. Therefore, 79 patients were included in this study.

MR imaging

Imaging studies were performed on a 3.0 T MRI system (Achieva 3.0 T; Philips Medical Systems, Best, Netherlands) before clinical intervention. A body coil was used for radiofrequency (RF) transmission, and a 16-channel head coil was used for signal reception. Conventional MR images were acquired according to the routine brain tumor protocol in our hospital and included axial T_1-weighted imaging (repetition time (ms)/echo time (ms), 400/20), axial T_2-weighted imaging (repetition time (ms)/echo time (ms), 2800/105), and axial fluid-attenuated inversion recovery (FLAIR) imaging (repetition time (ms)/echo time (ms)/inversion recovery time (ms) 8000/204/2200). Then, axial, coronal and sagittal gadolinium-enhanced T_1-weighted images were obtained after a contrast agent (Gd-DTPA; 0.2 ml/kg body weight; Magnevist; Bayer Schering, Guangzhou, China) was injected. Other imaging parameters were as follows: field of view, 240×240 mm^2; slice thickness, 5 mm; gap, 2 mm; and matrix, 512×512. The 2D fat-suppressed, fast spin-echo APTw pulse sequence was performed at one T_2-weighted image slice showing the maximum area of the tumor before the Gd-T_1-weighted image. The APTw images were acquired with a multi-offset (offsets=0, ±0.25, ±0.5, ±0.75, ±1, ±1.5, ±2, ±2.5, ±3, ±3.25, ±3.5, ±3.75, ±4, ±4.5, ±5 and ±6 ppm), multi-acquisition protocol with a pulse-train radiofrequency saturation (duration time=800 ms; inter-pulse delay=10 ms; power level=2 μT). The protocol was repeated 8 times at an offset of ±3.5 ppm to increase the signal-to-noise ratio of the APTw images. In addition, an image that did not exert a saturated pulse was acquired for signal normalization, and an image that exerted a saturated pulse at the offset of 15.6 ppm was acquired to calculate the conventional magnetization transfer ratio (MTR) value. The detailed imaging parameters were as follows: sensitivity-encoding facto r=2, repetition time=3 s; echo time=11 ms; field of view, 240×240 mm^2; section thickness=6 mm; matrix=128×64; and voxel size=1.65×3.15×6.00 mm^3. The total acquisition time was 192 s.

Image analysis

The APTw raw data were analyzed using interactive data language written in the IDL program (Research Systems, Inc., Boulder, CO, USA). First, the normalized saturated signal intensity curve (S_{sat}/S_0, where S_{sat} and S_0 were the signal intensities obtained with and without selective saturation, respectively), known as the Z-spectrum, was calculated as a function of the saturation frequency offset. As described previously [26], the B_0 field inhomogeneity effect was corrected. To reduce the contributions from conventional

magnetization, transfer contrast and direct saturation of bulk water, a B_0-corrected Z-spectrum was used to analyze the magnetization transfer ratio asymmetry (MTR_{asym}) as follows: $MTR_{asym}=S_{sat}(-\text{off set})/S_0-S_{sat}(+\text{offset})/S_0$. The APTw signal was calculated as $MTR_{asym}(3.5\ ppm)$.

Two experienced neuroradiologists (X.W. and S.J., who had 11 and 10 years of experience in neuroradiology, respectively) analysis the conventional and APTw images. According to previous study[27], the tumor signal intensity on T_1- and T_2-weighted image, tumor enhancement type on gadolinium-enhanced T_1-weighted image and tumor volume were recorded, we also calculated the edema index (EI) which defined as $EI=V_{tumor+edema}/V_{tumor}$[28]. Five regions of interest (ROIs) were distributed based on the Gd-T_1WI and T_2WI co-registered with the APTw image[29], the size of each ROI was fixed at 15 pixels (Fig. 1). Necrosis, cystic cavities, large vessels, calcification and hemorrhagic components were excluded. For each patient, the APTw values in five ROIs ($APTw_1$,$APTw_2$…$APTw_5$) were recorded. Then, the maximum APTw value of them ($APTw_{max}$), the minimum APTw value of them ($APTw_{min}$), the maximum APTw value-minimum APTw value ($APTw_{max-min}$) and ($APTw_1+APTw_2+…+APTw_5$)/5 ($APTw_{mean}$) were determined.

Pathological data acquisition

The neurosurgeon (S.Z. who had 25 years of experience in neurosurgery) obtained specimens from the tumor region that showed the highest signal on APTw imaging during surgery. One neuropathologist (Y.L. who had 6 years of experience in neuropathology) reviewed specimens after hematoxylin and eosin (H & E) and Ki-67 antigen staining and pathological diagnosis was made based on the 2016 World Health Organization(WHO) classification of tumors of the central nervous system(CNS). For diagnosis WHO grade II meningioma, the following criterias are used, 4 to 19 mitoses per 10 high-power fields (HPF), the presence of brain invasion, or the presence of at least 3 of other 5 features: sheet-like growth, loss of whirling or fascicular architecture, hypercellularity, prominent nucleoli, spontaneous necrosis and tumor clusters with high nuclear to cytoplasmic ratio (N/C). [30],Additionally, the Ki-67 labeling index was estimated.

Statistical analysis

Statistical analyses were performed using a statistical analysis software (SPSS 19.0). The patient's gender, tumour signal intensity and enhancement type on conventional MRI between WHO grade I and grade IIusing the chi-square test. The comparisons between patient's age, tumour volume, EI, $APTw_{max}$, $APTw_{min;}$ $APTw_{max}$-$APTw_{min}$, $APTw_{mean}$ values and the Ki-67 labeling index for grade I and grade II tumors were performed using an independent samples *t*-test, followed by the Levene test. Receiver operating characteristic (ROC) curves were generated for each APTw parameter value to assess the areas under the curve (AUCs) and determine the optimal cut-off values for discrimination between two clinical entities. AUC values of <0.7, 0.7–0.9 and>0.9 indicated low, medium and high diagnostic performance, respectively. Logistic regression was applied to evaluate the diagnostic performance of the combination indices. Pearson's correlation coefficient was used to analyze the association between $APTw_{max}$ and Ki-67 labeling index of all

meningioma. Linear regression equation was established to evaluate the Ki-67 labeling index. $P<0.05$ was considered to be a statistically significant difference for all tests.

Results

53 patients were pathologically diagnosed with WHO grade I meningioma (21 males, 32 females; age range, 19–73 years; mean age, 48.9±12.3 years), included 19 fibroblastic, 20 meningothelial, 9 transitional, and 5 microcystic meningiomas. (23/53) cases found psammoma bodies. 26 patients were pathologically diagnosed with WHO grade II meningioma (11 males, 15 females; age range, 18–67 years; mean age, 53.2±11.3 years), included 23 atypical, 2 clear-cell and 1 chordoid meningiomas. (5/26) cases found psammoma bodies.

The gender ratio and age was not significantly different between WHO grade I and WHO grade II meningiomas (*P=0.947* and *P=0.095,* respectively). The proliferation index in grade II meningiomas was significantly higher than in grade I tumors (5.85%±3.18% vs. 4.06% ±2.31%, *P=0.015*).

For 53 cases WHO grade I meningiomas, (17/53) cases showed hypointense and (36/53) cases showed isointense on T_1-weighted image, (3/53) cases showed hypointense (21/53) cases showed isointense and (29/53) cases showed hyperintense on T_2-weighted image, On the Gd-T_1W image, (42/53) cases showed homogenous enhancement and (11/53) showed heterogeneous enhancement. The tumour volume range from 28.3–40.8 mm^3, When the quantitative EI was measured, 21 cases were EI≤1.5, 28 cases 1.5<EI≤3, and 4 cases EI>3. For 26 cases of WHO grade II meningiomas, (12/26) cases showed hypointense and (14/26) cases showed isointense on T_1-weighted image. (1/26) cases showed hypointense, (8/26) cases showed isointense and (17/26) cases showed hyperintense on T_2-weighted image. On the Gd-T_1-weighted image, (12/26) cases showed homogenous enhancement and (14/26) showed heterogeneous enhancement. The tumour volume range from 31.8–41.2 mm^3. When the quantitative EI was measured, 6 cases were EI ≤1.5, 18 cases 1.5<EI≤3, and 2 cases EI>3. No significant difference in tumoral signal on T_1 and T_2-weighted image (*P=0.320*, *P=0.661* respectively), tumoral volume (35.2 mm^3 ±5.2 mm^3 vs. 36.7 mm^3 ±4.5 mm^3, *P=0.149*) and EI value (1.70±0.86 vs. 2.01±0.71, *P=0.119*) between WHO grade I and WHO grade II tumors. However, WHO grade II meningiomas showed heterogeneous enhancement than grade I meningiomas(*P=0.004*).

Both WHO grade I and WHO grade II meningiomas identified by APTw imaging was approximately equal to that identified on the Gd-T_1 weighted images. Compared with the CNAWM, for (12/53) WHO grade I meningiomas cases, the Gd-enhancing tumor parenchyma showed heterogeneous signal on APTw images(Fig. 2). for (41/53) WHO grade I meningiomas cases, the Gd-enhancing tumor parenchyma overall showed hyperintense on APTw images, within them, (5/41) meningiomas showed more homogeneous hyperintense than their partners, Interestingly, 5 meningiomas were confirmed as microcystic meningiomas by pathology.(Fig. 3) Compared with the CNAWM, for (26/26) WHO grade II meningiomas cases, the Gd-enhancing tumor parenchyma overall showed homogeneous hyperintense on APTw images(Fig. 4).

The values of the APTw parameters for the two groups are summarized in Table 1. No significant differences in $APTw_{max}$ value (*P=0.103*) and $APTw_{mean}$ value (*P=0.318*) were identified between the WHO grade I and WHO grade II tumors. The $APTw_{min}$ values was higher in WHO grade II meningiomas than in WHO grade I tumors (*P=0.027*). The $APTw_{max-min}$ values was lower in WHO grade II meningiomas than in WHO grade I meningiomas (*P=0.019*). However, the $APTw_{min}$ was higher and the $APTw_{max-min}$ was lower in 5 cases microcystic meningiomas than in WHO grade II meningiomas(*P=0.001* and *P=0.006*).

The diagnostic performance of APTw parameters in prediction the grade of meningiomas are summarized in Table 2. It was showed that $APTw_{min}$ combined with $APTw_{max-min}$ had the highest AUC of 0.772,(Fig. 5) when the $APTw_{min}$ higher than 2.58% combined with $APTw_{max-min}$ lower than 0.89%, the lesion was diagnosed as an WHO grade II, the sensitivity was 67.9%, the specificity was 96.2%.

The $APTw_{max}$ value was positively correlated with Ki-67 labeling index in meningiomas (r=0.817, *P*<0.001). The regression equation for the Ki-67 labeling index(%) (Y) and $APTw_{max}$ (%) (X) among meningiomas was $Y=4.9\times X-12.4$ ($R^2=0.667$, P<0.001). According to the regression equation, the $APTw_{max}$ value was 3.14% when the Ki-67 labeling index was 3%.

Discussion

Consistent with Lin's report[27], both of the group had a female predominance and hererogeneous enhancement was more common in WHO grade II meningiomas in this study. Lin reported that high-grade meningiomas were more common in older, that is not supported by this study, maybe it was result of the bias of the sample. Consistent with Soon's report[31], the tumour volume of WHO grade II meningiomas were not significantly higher than grade I meningiomas. Additionally, Soon found grade II meningioma have significantly higher volumetric growth rate than grade I meningioma, the statement was not discussed in this study. The EI was not different between WHO grade I and grade II meningiomas, because peritumoral edema in meningiomas was depend on AQP-4 expression and the expression of AQP-4 was not related with tumor grade [32].

Compared with CNAWM, both WHO grade I and grade II meningiomas showed completely hyperintense or hyperintense mixed with isointense on APTw images. The lesions identified by APTw were approximately equal to those identified by Gd-T_1W images. Technically, the predominantly factors affect the APTw signal was cell density and mobile amide proton[26], the tumor core had greater cell densities and mobile protein and peptide content than in CNAWM, This finding was particularly valuable for the meningioma patients without proper surgical indications, because potential central nervous system damage and nephrogenic systemic fibrosis caused by Gd deposition may be missed upon re-examination[33; 34].

For the meningiomas which demonstrated isointense on APTw images, we found they were richer in psammoma bodies, and the isointense region more larger, the psammoma bodies content more richer, maybe the psammoma bodies generate weaker APT effect. It was useful

for predicting the hardness of the meningioma, because the psammoma bodies content more richer and the masses were more harder, then the tumor would be more difficult to remove, it was helpful in making surgical plans.

The $APTw_{max}$ and $APTw_{mean}$ values of WHO grade II meningiomas were not statistically higher than grade I meningiomas. Pathologically, compared with WHO grade I meningiomas, the grade II meningiomas were associated with a higher cell density and N/C ratio[30]. According to previous studies, Technically, higher cell density made WHO grade II generate stronger APT effect than WHO grade I meningioma, However, higher N/C ratio made WHO grade II generate weaker APT effect than WHO grade I meningioma[13; 26]. perhaps this lead to an overlap between the APTw signal of meningiomas in different grade. The $APTw_{min}$ value was lower in grade I meningiomas. Pathologically, compared to WHO grade I meningiomas the psammoma bodies which supposed to generate poor APT effect were more common in grade I meningiomas. As a parameter that indicated the APTw signal heterogeneity, the $APTw_{max-min}$ was lower in the WHO grade meningioma than in the WHO grade I meningioma. Pathologically, In WHO grade I meningioma, the shapes of the neoplastic cells were oval or spindle-shaped and formed whorls, fascicles, cords or nodules. By contrast, specific patterns were rarely found in WHO grade I meningiomas[30]. Perhaps the special pathological structure resulted in more uneven distribution of mobile protein and peptide content in low-grade meningiomas than in their high-grade partners. According to ROC analysis, even $APTw_{min}$ combine with $APTw_{max-min}$ has the best diagnostic performance in prediction the grade of meningioma, but the sensitivity and specificity was only 67.9% and 96.2%, the performance of APTw-MRI used for grading meningiomas was not as good as in glioma[15]. Maybe, the meningiomas components were more complex than glioma.

It is interesting that as WHO grade I meningiomas, the signal features of microcystic meningiomas were similar with that of WHO grade II meningiomas on the APTw MR images; Quantify the APTw parameters, the $APTw_{min}$ of microcystic meningioma was higher and the $APTw_{max-min}$ was lower than that of grade II meningiomas. Histologically, numerous microcysts spaces formed by tumor cells and extracellular substrates in microcystic meningiomas, and the spaces filled with edematous fluid [35]. Maybe the mobile protein and peptide content in microcystic meningiomas are higher and the distribution more homogeneous than high-grade meningioma. We hypothesize that beside the grade of the meningiomas, the subtype of the meningioma affect the APTw signal either, and additional study is needed.

Compared with studies in gliomas using APTw-MRI[36; 37], we found that $APTw_{max}$ was positively correlated with Ki-67 labeling index in meningiomas either. According to the one-dimensional linear regression equation, when the $APTw_{max}$ value is higher than 3.14%, Ki-67 labeling index is 3%, and thus, more enterprising presurgical planning should be considered.

This study had some limitations. First, there were only 7 subtypes of meningiomas and no WHO grade III meningiomas were recruited. Further exploration is needed to clarify the link between APTw parameters and grade or subtypes as more cases and subtypes of

meningiomas are recruited. Second, the APTw sequence covered only one slice; as the 3D-APTw MRI developed, additional cases will recruit using the 3D-APTw sequence to assess tumors comprehensively. Third, the neurosurgeon obtained the samples from target part according to his experience, so there was potential bias in acquisition the specimens; in the future, we will request the neurosurgeon take measure to obtain more accurate samples.

In conclusion, the APTw-MR imaging used to differentiating the grades of meningiomas are limited, beside the grade of the meningioma, the subtypes also influence the APT signal, and $APTw_{max}$ positively correlated with the Ki-67 proliferation status. Even the diagnostic performance was not good enough. As a supplementary MR technology, APT-weighted MRI would be providing a more comprehensive preoperative assessment of meningioma patients to benefit therapeutic decision making in the clinic.

Funding:

This study is partially supported by grants from Natural Science Foundation of Guangdong Province (2014A030313271), Guangdong Provincial Science and Technology Project (2014A020212726), Southern Medical University clinical research project (LC2016ZD028) and the National Institutes of Health (R01EB009731, R01CA166171).

Guarantor:

The scientific guarantor of this publication is Zhibo Wen Ph.D., M.D.

Abbreviations:

APT	amide proton transfer
APTw	APT-weighted
CEST	chemical exchange-based saturation transfer
CNAWM	contralateral normal-appearing white matter
Gd	gadolinium
H&E	hematoxylin and eosin
N/C	nucleus to cytoplasm ratio
ROI	region of interest

References

1. Ostrom QT, Gittleman H, Liao P, et al. (2017) CBTRUS Statistical Report: Primary brain and other central nervous system tumors diagnosed in the United States in 2010–2014. Neuro-oncology 19:vl–v88
2. Kshettry VR, Ostrom QT, Kruchko C, Al-Mefty O, Barnett GH, Barnholtz-Sloan JS (2015) Descriptive epidemiology of World Health Organization grades II and III intracranial meningiomas in the United States. Neuro-oncology 17:1166–1173 [PubMed: 26008603]
3. Lin Z, Zhao M, Ren X, et al. (2017) Clinical Features, Radiologic Findings, and Surgical Outcomes of 65 Intracranial Psammomatous Meningiomas. World neurosurgery 100:395–406 [PubMed: 28132920]

4. Swiderska-Chadaj Z, Markiewicz T, Grala B, Lorent M (2016) Content-based analysis of Ki-67 stained meningioma specimens for automatic hot-spot selection. Diagnostic pathology 11:93 [PubMed: 27717363]
5. Marciscano AE, Stemmer-Rachamimov AO, Niemierko A, et al. (2016) Benign meningiomas (WHO Grade I) with atypical histological features: correlation of histopathological features with clinical outcomes. Journal of neurosurgery 124:106–114 [PubMed: 26274991]
6. Lu Y, Xiong J, Yin B, Wen J, Liu L, Geng D (2018) The role of three-dimensional pseudo-continuous arterial spin labelling in grading and differentiating histological subgroups of meningiomas. Clinical radiology 73:176–184 [PubMed: 29031810]
7. Xing F, Tu N, Koh TS, Wu G (2017) MR diffusion kurtosis imaging predicts malignant potential and the histological type of meningioma. European journal of radiology 95:286–292 [PubMed: 28987682]
8. Zikou A, Alexiou GA, Goussia A, et al. (2016) The role of diffusion tensor imaging and dynamic susceptibility perfusion MRI in the evaluation of meningioma grade and subtype. Clinical neurology and neurosurgery 146:109–115 [PubMed: 27208870]
9. Surov A, Ginat DT, Sanverdi E, et al. (2016) Use of Diffusion Weighted Imaging in Differentiating Between Maligant and Benign Meningiomas. A Multicenter Analysis. World neurosurgery 88:598–602 [PubMed: 26529294]
10. Surov A, Gottschling S, Mawrin C, et al. (2015) Diffusion-Weighted Imaging in Meningioma: Prediction of Tumor Grade and Association with Histopathological Parameters. Translational oncology 8:517–523 [PubMed: 26692534]
11. Santelli L, Ramondo G, Della Puppa A, et al. (2010) Diffusion-weighted imaging does not predict histological grading in meningiomas. Acta neurochirurgica 152:1315–1319; discussion 1319 [PubMed: 20428902]
12. Zhou J, Payen JF, Wilson DA, Traystman RJ, van Zijl PC (2003) Using the amide proton signals of intracellular proteins and peptides to detect pH effects in MRI. Nature medicine 9:1085–1090
13. Jiang S, Yu H, Wang X, et al. (2016) Molecular MRI differentiation between primary central nervous system lymphomas and high-grade gliomas using endogenous protein-based amide proton transfer MR imaging at 3 Tesla. European radiology 26:64–71 [PubMed: 25925361]
14. Togao O, Kessinger CW, Huang G, et al. (2013) Characterization of lung cancer by amide proton transfer (APT) imaging: an in-vivo study in an orthotopic mouse model. PloS one 8:e77019 [PubMed: 24143199]
15. Zou T, Yu H, Jiang C, et al. (2018) Differentiating the histologic grades of gliomas preoperatively using amide proton transfer-weighted (APTW) and intravoxel incoherent motion MRI. NMR in biomedicine 31
16. Togao O, Yoshiura T, Keupp J, et al. (2014) Amide proton transfer imaging of adult diffuse gliomas: correlation with histopathological grades. Neuro-oncology 16:441–448 [PubMed: 24305718]
17. Ma B, Blakeley JO, Hong X, et al. (2016) Applying amide proton transfer-weighted MRI to distinguish pseudoprogression from true progression in malignant gliomas. Journal of magnetic resonance imaging : JMRI 44:456–462 [PubMed: 26788865]
18. Zhou J, Tryggestad E, Wen Z, et al. (2011) Differentiation between glioma and radiation necrosis using molecular magnetic resonance imaging of endogenous proteins and peptides. Nature medicine 17:130–134
19. Yu H, Lou H, Zou T, et al. (2017) Applying protein-based amide proton transfer MR imaging to distinguish solitary brain metastases from glioblastoma. European radiology 27:4516–4524 [PubMed: 28534162]
20. Dula AN, Arlinghaus LR, Dortch RD, et al. (2013) Amide proton transfer imaging of the breast at 3 T: establishing reproducibility and possible feasibility assessing chemotherapy response. Magnetic resonance in medicine 70:216–224 [PubMed: 22907893]
21. Jia G, Abaza R, Williams JD, et al. (2011) Amide proton transfer MR imaging of prostate cancer: a preliminary study. Journal of magnetic resonance imaging : JMRI 33:647–654 [PubMed: 21563248]

22. Zhang H, Kang H, Zhao X, et al. (2016) Amide Proton Transfer (APT) MR imaging and Magnetization Transfer (MT) MR imaging of pediatric brain development. European radiology 26:3368–3376 [PubMed: 26762941]
23. Tietze A, Blicher J, Mikkelsen IK, et al. (2014) Assessment of ischemic penumbra in patients with hyperacute stroke using amide proton transfer (APT) chemical exchange saturation transfer (CEST) MRI. NMR in biomedicine 27:163–174 [PubMed: 24288260]
24. Li C, Peng S, Wang R, et al. (2014) Chemical exchange saturation transfer MR imaging of Parkinson's disease at 3 Tesla. European radiology 24:2631–2639 [PubMed: 25038850]
25. Joo B, Han K, Choi YS, et al. (2018) Amide proton transfer imaging for differentiation of benign and atypical meningiomas. European radiology 28:331–339 [PubMed: 28687916]
26. Wen Z, Hu S, Huang F, et al. (2010) MR imaging of high-grade brain tumors using endogenous protein and peptide-based contrast. Neuroimage 51:616–622 [PubMed: 20188197]
27. Lin BJ, Chou KN, Kao HW, et al. (2014) Correlation between magnetic resonance imaging grading and pathological grading in meningioma. Journal of neurosurgery 121:1201–1208 [PubMed: 25148010]
28. Osawa T, Tosaka M, Nagaishi M, Yoshimoto Y (2013) Factors affecting peritumoral brain edema in meningioma: special histological subtypes with prominently extensive edema. Journal of neuro-oncology 111:49–57 [PubMed: 23104516]
29. Zhang Y, Heo HY, Lee DH, et al. (2016) Selecting the reference image for registration of CEST series. Journal of magnetic resonance imaging : JMRI 43:756–761 [PubMed: 26268435]
30. Louis DN, Perry A, Reifenberger G, et al. (2016) The 2016 World Health Organization Classification of Tumors of the Central Nervous System: a summary. Acta neuropathologica 131:803–820 [PubMed: 27157931]
31. Soon WC, Fountain DM, Koczyk K, et al. (2017) Correlation of volumetric growth and histological grade in 50 meningiomas. Acta neurochirurgica 159:2169–2177 [PubMed: 28791500]
32. Gawlitza M, Fiedler E, Schob S, Hoffmann KT, Surov A (2017) Peritumoral Brain Edema in Meningiomas Depends on Aquaporin-4 Expression and Not on Tumor Grade, Tumor Volume, Cell Count, or Ki-67 Labeling Index. Molecular imaging and biology : MIB : the official publication of the Academy of Molecular Imaging 19:298–304 [PubMed: 27552812]
33. Collidge TA, Thomson PC, Mark PB, et al. (2007) Gadolinium-enhanced MR imaging and nephrogenic systemic fibrosis: retrospective study of a renal replacement therapy cohort. Radiology 245:168–175 [PubMed: 17704357]
34. Ramalho J, Castillo M, AlObaidy M, et al. (2015) High Signal Intensity in Globus Pallidus and Dentate Nucleus on Unenhanced Tl-weighted MR Images: Evaluation of Two Linear Gadolinium-based Contrast Agents. Radiology 276:836–844 [PubMed: 26079490]
35. Seok JY, Kim NR, Cho HY, Chung DH, Yee GT, Kim EY (2014) Crush cytology of microcystic meningioma with extensive sclerosis. Korean journal of pathology 48:77–80 [PubMed: 24627702]
36. Bai Y, Lin Y, Zhang W, et al. (2017) Noninvasive amide proton transfer magnetic resonance imaging in evaluating the grading and cellularity of gliomas. Oncotarget 8:5834–5842 [PubMed: 27992380]
37. Su C, Liu C (2017) Amide Proton Transfer Imaging Allows Detection of Glioma Grades and Tumor Proliferation: Comparison with Ki-67 Expression and Proton MR Spectroscopy Imaging. 38:1702–1709

Key Points

- The $APTw_{min}$ value was higher and the $APTw_{max-min}$ value was lower in WHO grade II meningioma than in grade I tumors.
- the $APTw_{min}$ value was higher and the $APTw_{max-min}$ value was lower in microcystic meningiomas than WHO grade II meningiomas
- The $APTw_{max}$ value was positively correlated with meningioma proliferation index

Methodology:

- retrospective
- diagnostic or prognostic study
- performed at one institution

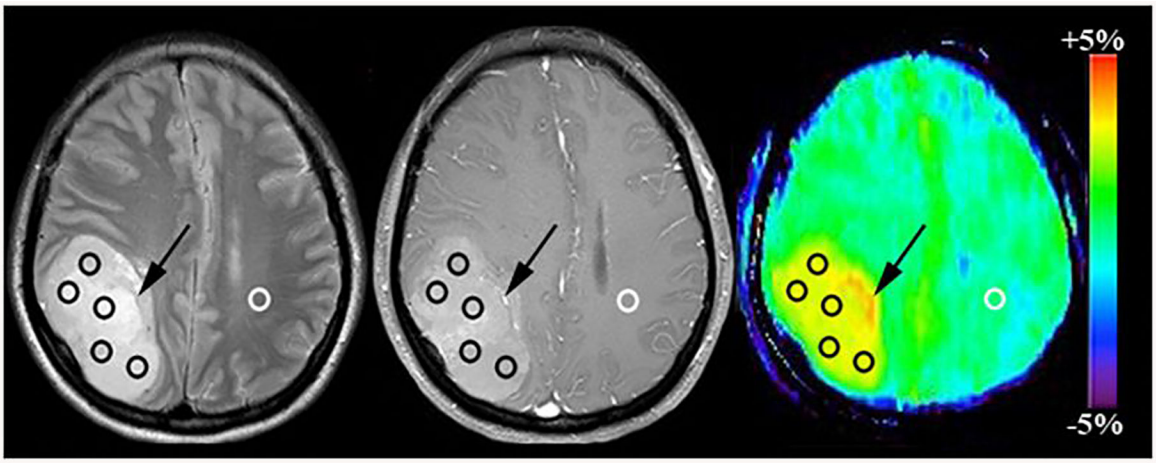

Fig. 1:
Example of the placement of ROIs. Five ROIs were placed in the Gd-enhancing tumour part (Black Circle) and one ROI was placed in the CNAWM (White Circle) based on the co-registered traditional images The vessel-related image artefact can be seen. (Black arrow).

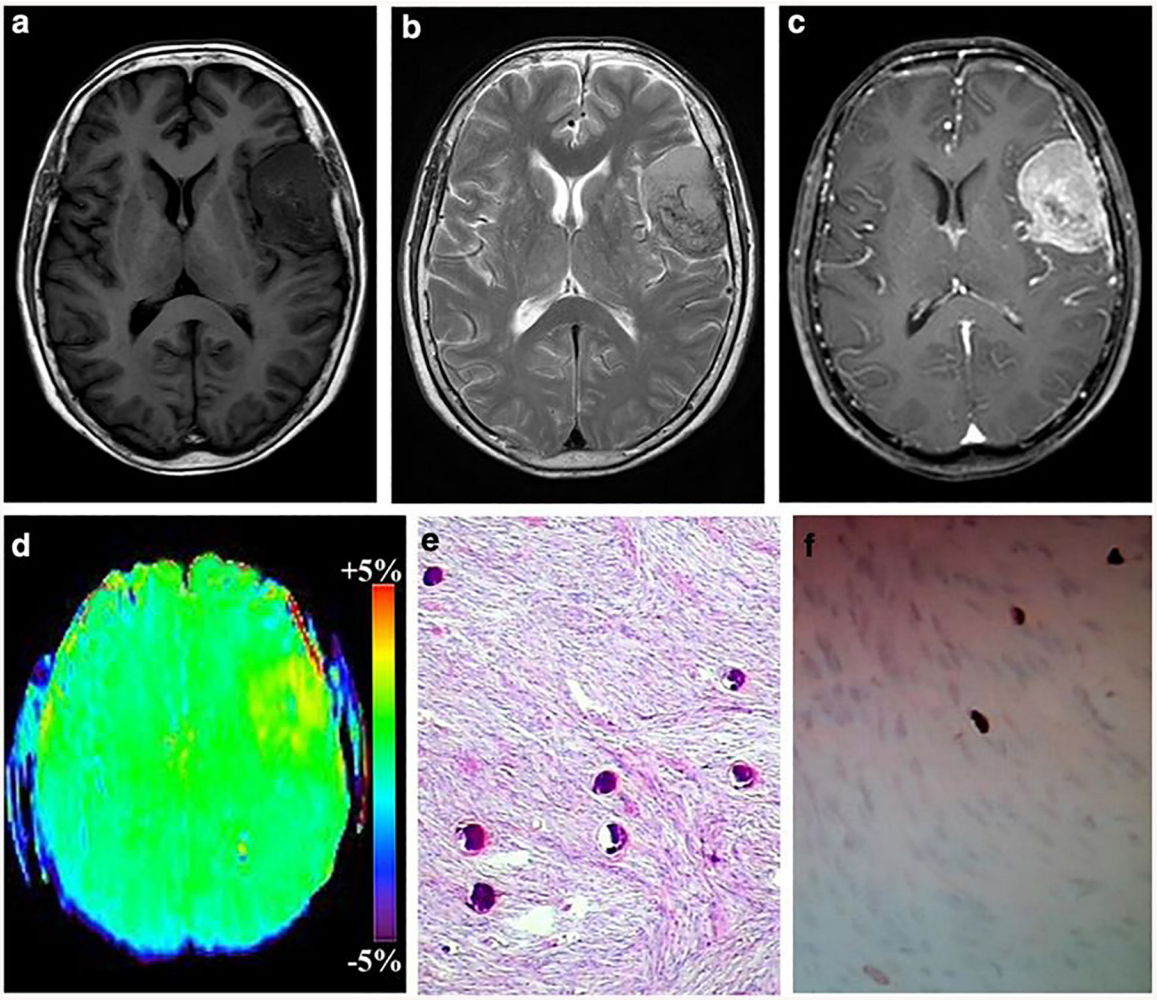

Fig. 2:

A 39-year-old male with fibroblastic meningioma (WHO grade I). a-c The mass was located in the left frontal, it exhibiting isointense on T_1WI, hyperintense on T_2WI and heterogeneous enhancement, d On APTw image, the mass exhibiting heterogeneous signal and the tumor identified approximately equal as on the Gd-T_1weighted images, the $APTw_{max}$= 3.18%, $APTw_{min}$= 2.06% $APTw_{max-min}$= 1.12%, $APTw_{mean}$= 2.63%. The part rich in psammoma body showed hypointense on T_1WI and T_2WI, and isointense on APTw image. (Black arrow) e HE staining showed many psammoma body in the tumor, f Ki-67 labeling index was 3%.

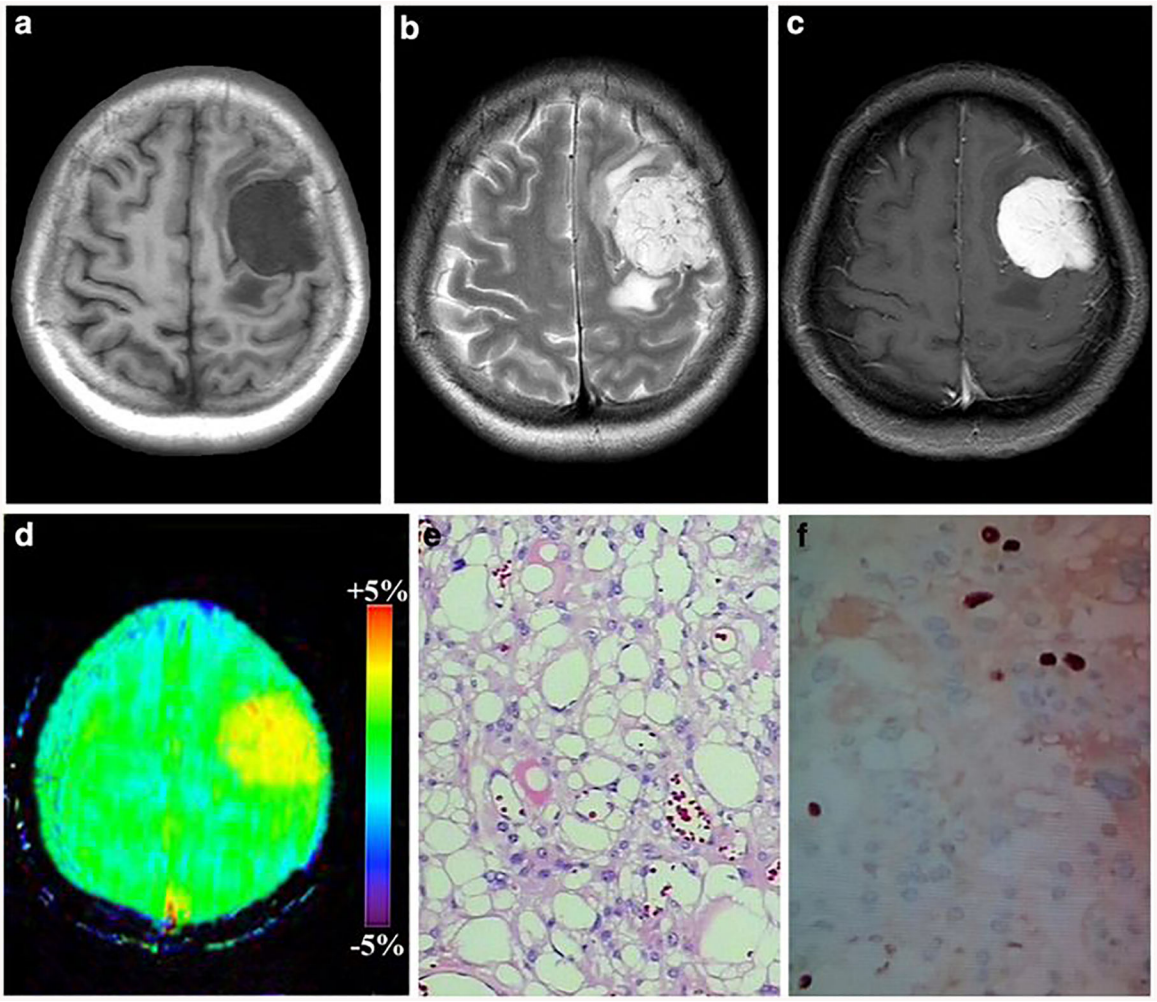

Fig. 3:

A 54-year-old female with microcystic meningioma (WHO grade I). a-c The mass was located in the left frontal, it exhibiting hypointense on T_1WI, hyperintense on T_2WI and obvious homogeneous enhancement, d On APTw image, the mass exhibiting homogeneous signal and the tumor identified approximately equal as on the Gd-T_1weighted images. $APTw_{max}$= 3.58%, $APTw_{min}$= 3.22% $APTw_{max\text{-}mn}$= 0.36%, $APTw_{mean}$= 3.45%. e HE staining showed numerous microcysts spaces in the tumor, f Ki-67 labeling index was 5%.

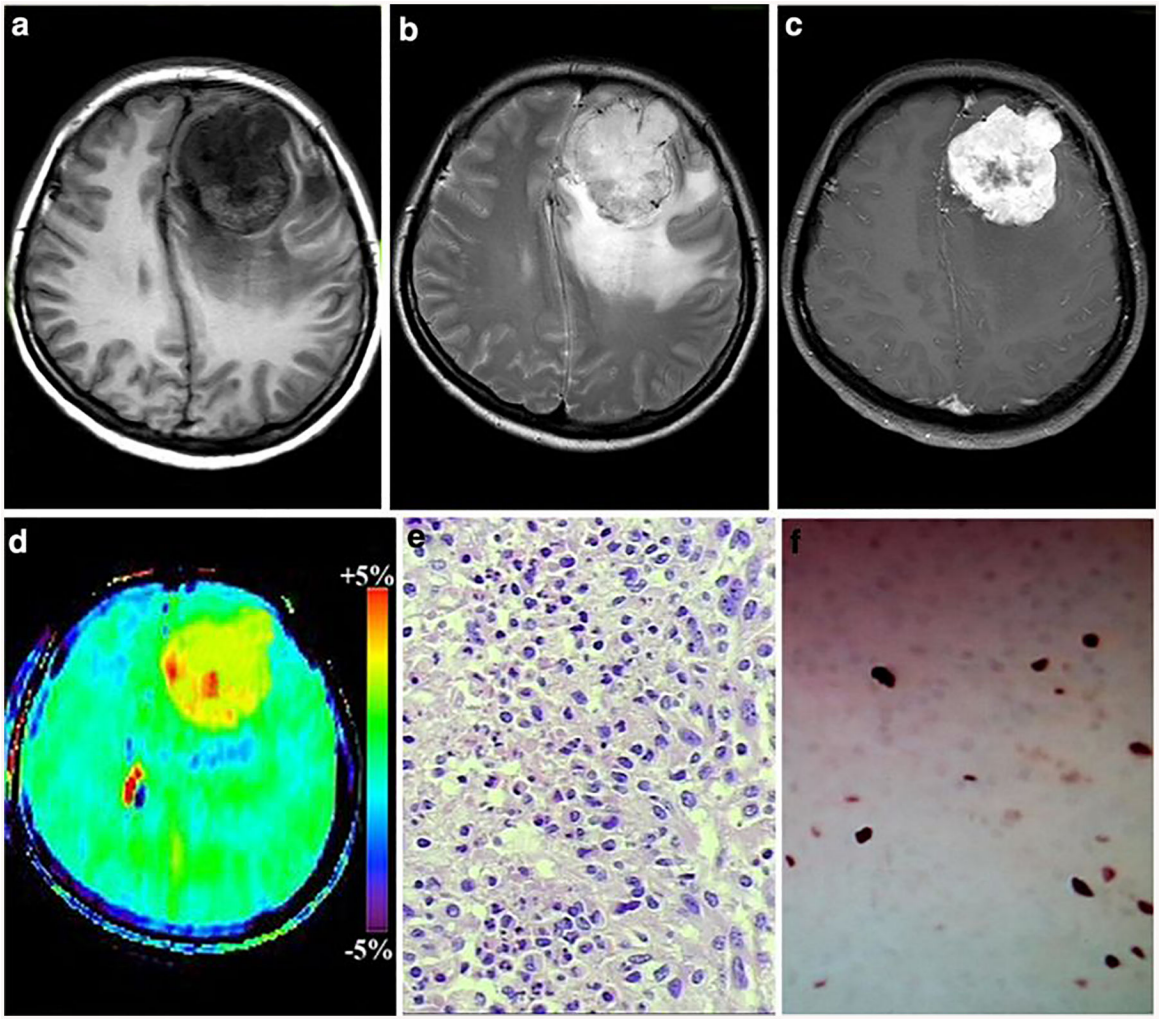

Fig. 4:

A 49-year-old female with atypical meningioma (WHO grade II). a-c The mass was located in the left frontal, it exhibiting hypointense on T_1WI, hyperintense on T_2WI and obvious heterogeneous enhancement, d On APTw image, the mass exhibiting relative homogeneous signal and the tumor identified approximately equal as on the Gd-Ti weighted images the $APTw_{max}$= 4.02%, $APTw_{min}$= 3.11% $APTw_{max\text{-}min}$= 0.71%, $APTw_{mean}$= 3.87%). Necrosis-related image artefact (Black arrow) and ventricle-related image artefact (White arrow) can be seen.e HE staining showed high nuclear to cytoplasmic ratio cells are arranged loss of whirling or fascicular architecture, f Ki-67 labeling index was 10%).

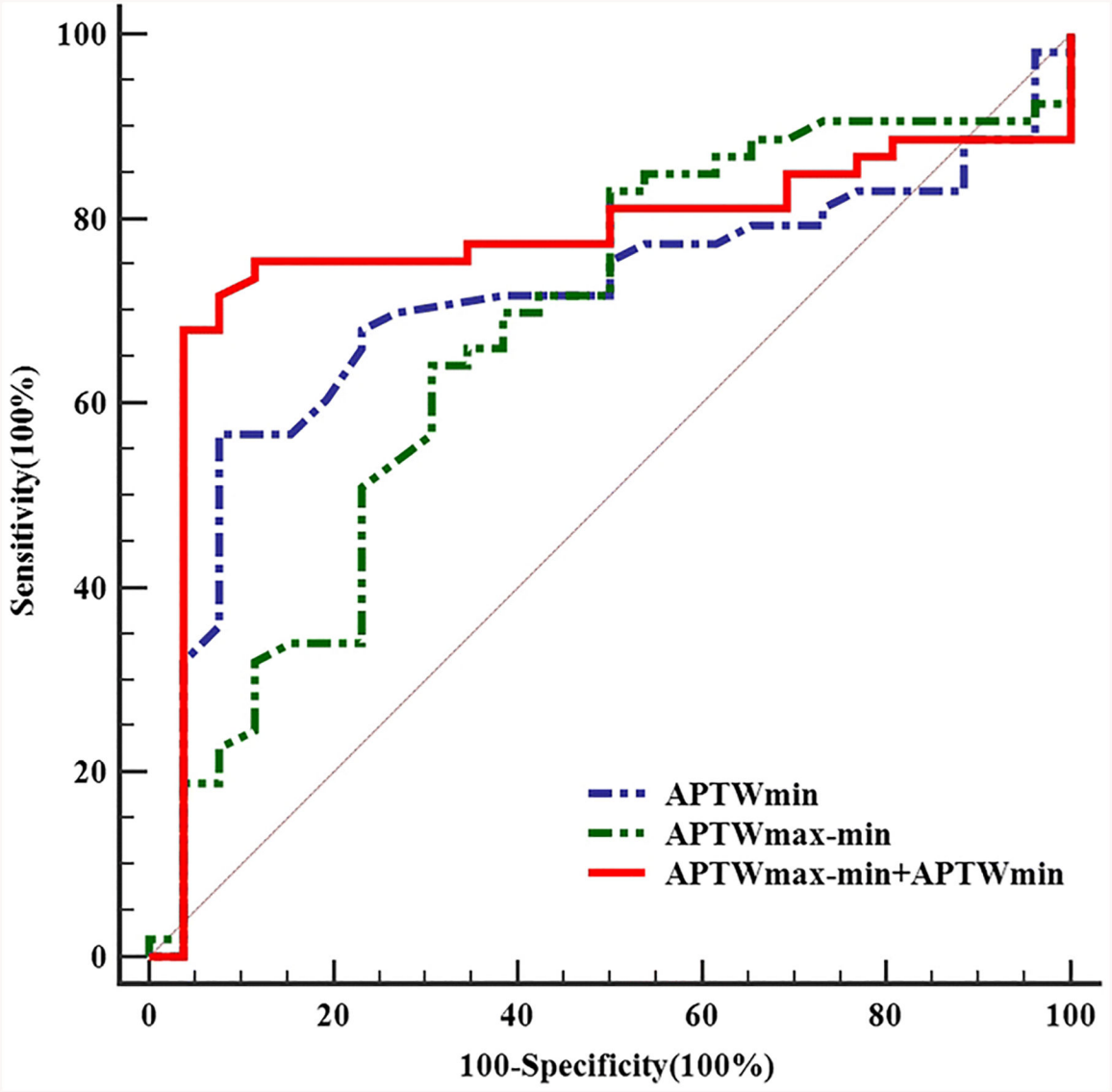

Fig. 5. Diagnostic performance of amide proton transfer (APT) parameters in differentiating the grade of meningioma.

$APTw_{min}$ combined with $APTw_{max-min}$ showed the best diagnostic performance, with an AUC of 0.772, followed by $APTw_{max-min}$ of 0.708 and $APTw_{min}$ of 0.673.

Table 1

Comparing difference of APTw within WHO grade I and WHO grade II meningiomas

	WHO grade I	WHO grade II	*P*
$APTw_{max}$ (%)	3.39±0.45	3.57±0.44	***0.103***
$APTw_{min}$ (%)	2.50±0.49	2.77±0.47	***0.027***
$APTw_{mean}$ (%)	3.06±0.45	3.17±0.47	***0.318***
$APTw_{max-min}$ (%)	0.89±0.19	0.78±0.16	***0.019***

Abbreviations: $APTw_{max}$, amide proton transfer-weighted max; $APTw_{min}$, amide proton transfer-weighted min; $APTw_{mean}$ amide proton transfer-weighted mean; $APTw_{max-min}$, amide proton transfer-weighted max-amide proton transfer-weighted min

Table 2

Diagnostic performance of APTw parameters in prediction the grade of meningioma

	Cut-off value	Sensitivity(%)	Specificity(%)	AUC
$APTw_{min}$	2.58	64.2	69.2	0.673
$APTw_{max-min}$	0.89	56.6	92.3	0.708
$APTw_{min}$+$APTw_{max-min}$	-[a]	67.9	96.2	0.772

Abbreviations: $APTw_{min}$, amide proton transfer-weighted min; $APTw_{max-min}$, amide proton transfer-weighted max-amide proton transfer-weighted min; AUC, area under the curve

[a]The combined cut-off values were the same as the individual index above